Biocidal Organotin Compounds. Part 2. Synthesis, Characterization and Biocidal Properties of Triorganotin(IV) Hydantoic Acid Derivatives and the Crystal Structures of Triphenyltin- and Tricyclohexyltin- Hydantoate

Sk. Kamruddin,* T.K. Chattopadhyaya,* A. Roy,* and E.R.T. Tiekink†

* Department of Chemistry, University of North Bengal, Darjeeling-734430, India,

† Department of Chemistry, The University of Adelaide, Adelaide, South Australia 5005, Australia.

The preparation and spectroscopic (^{1}H NMR, UV and IR) characterization of three $R_3Sn(O_2CCH_2N(H)C(O)NH_2)$, R = Ph, c-Hex or nBu, compounds is reported. A different mode of coordination is indicated for the hydantoate ligand in the R = Ph compound compared with the R = c-Hex and R = nBu compounds as confirmed by a crystallographic analysis. The structure of $[Ph_3Sn(O_2CCH_2N(H)C(O)NH_2)]$ is polymeric owing to the presence of bridging hydantoate ligands such that each ligand coordinates one tin atom

via one of the carboxylate oxygen atoms and a symmetry related tin atom via the carbonyl group of the other end of the molecule. The structure features distorted trigonal bipyramidal tin atom geometries with a <u>trans</u>-R_3SnO_2 motif. The structure of [c-$Hex_3Sn(O_2CCH_2N(H)C(O)NH_2)$] by contrast is monomeric, distorted tetrahedral as the carboxylate group is again monodentate and there are no additional tin-ligand interactions. The structures are each stabilized by a number of intermolecular hydrogen bonds. Fungitoxicity and phytotoxicity studies indicate that the R = nBu derivative is the more active compound.

Keywords: Triorganotin, carboxylate, crystal structure, fungitoxicity

---

INTRODUCTION

Various triorganotin carboxylates are known to have significant biocidal properties [1,2] and it is expected that the incorporation of biologically active entities into a triorganotin system would lead to the formation of potent biocides. Hydantoic acid, $H_2NC(O)N(H)CH_2C(O)OH$, and some of its derivatives are known to possess biological activity [3] and in the above context, its reactions with triorganotin moieties have been investigated in the present study. In addition to the carboxylate binding site, the anion derived from hydantoic acid has other potential donor sites available for coordination. Continuing previous work into the structure/activity relationship of organotin(IV) carboxylates,[4] the present report details a study of the interaction of triorganotin centres with hydantoic acid employing spectroscopic and crystallographic methods, as well as the biocidal properties of the new compounds.

EXPERIMENTAL

General

The solvents were purified and dried before use by standard procedures. Ph_3SnCl, $(nBu_3Sn)_2O$, c-Hex_3SnOH and hydantoic acid were used as received from commercial sources. Ph_3SnOH was prepared by alkaline hydrolysis of Ph_3SnCl.[5] The ^1H NMR spectra were recorded on a VA-EM-390 (90MHz) spectrometer. The IR spectra were recorded on a Pye-Unicam SP-300S spectrophotometer using CsI optics and UV spectra on a Shimadzu-240 spectrophotometer. Microanalyses were performed at RSIC, Punjab University and tin was estimated gravimetrically as SnO_2. Analytical data are presented in Table 1.

Syntheses

[$Ph_3Sn(O_2CCH_2N(H)C(O)NH_2)$]. A 250 ml round bottomed flask was placed on a heating mantle and fitted with a Dean-Stark apparatus with a double surface, water cooled reflux condenser. The entire apparatus was flushed with N_2 to exclude moisture and the reaction was carried out under N_2. Ph_3SnOH (1.4 g, 3.8 mmol), hydantoic acid (0.45 g, 3.8 mmol) and dry benzene (150 ml) were placed in the reaction vessel. The reaction was perfomed under reflux for 24 h with water produced being removed azeotropically. The resultant solution was concentrated and left to stand overnight. The white solid that precipitated was filtered off and washed successively with petroleum ether (60-80 °C) and chloroform. Recrystallization from methanol solution afforded colourless crystals. The other compounds were prepared using similar procedures; analytical data are given in Table 1.

Crystallography

Intensity data for colourless crystals were measured at room temperature on a Rigaku AFC6R diffractometer fitted with graphite monochromatized MoKα radiation, $\lambda = 0.71073$ Å, up to θ_{max} 27.5° employing the ω:2θ scan technique. The data were corrected for Lorentz and polarization effects [6] and for absorption employing the DIFABS program.[7] Of the data measured, those that satisfied the $I \geq 3.0\sigma(I)$ criterion of observability were used in the subsequent analysis. Crystal data are summarized in Table 2.

The structures were solved by direct methods [8] and each refined by a full-matrix least-squares procedure based on F.[6] Non-hydrogen atoms were refined with anisotropic thermal parameters and hydrogen-atoms were included in the models at their calculated positions (C-H, N-H 0.97 Å) with the following exception In the refinement of [c-$Hex_3Sn(O_2CCH_2N(H)C(O)NH_2)$], disorder (high thermal motion) was noted in the cyclohexyl ring C(31)-C(36) with two positions being detected for the C(36) atom; this

group was refined with isotropic thermal parameters and hydrogen atoms were not included. Final refinement details (sigma weights [6]) are listed in Table 2; the analysis of variance showed no special features in either case. The crystallographic numbering scheme used is shown in Figs 1 and 2 (drawn with ORTEP [9]) and fractional atomic coordinates are listed in Tables 3 and 4. Other crystallographic details comprising thermal parameters, hydrogen-atom parameters, all bond distances and angles, and tables of observed and calculated structure factors are available on request from ERTT.

Biological studies

The new compounds were screened for their antifungal effectiveness in vitro against Alternaria alternata (ITCC 3022), a causative organism of brown spot disease of tobacco, leaf spot and fruit rot of brinjal, Helminthosporium sativum (ITCC 2684), causal agent of spot blotch of wheat, Helminthosporium maydis (ITCC 2675), causal agent of brown spot of maize (zea mays), and Piricularia oryzae (ITCC 3050), blast disease of rice (oryzae sativa). The virulent cultures were obtained from the plant pathology laboratory, Department of Botany, U.N.B. Fungi were grown on potatoe-dextrose-agar (PDA) medium at 28 ± 1°C.

The fungicidal activities were determined following the spore germination method as described by Rouxel et al.[10] Eluents (10 µl) were placed on two spots 3 cm apart on a clean, grease-free slide and the solvent was allowed to evaporate. One drop of spore suspension (0.02 ml), prepared from 15-day-old culture was added to the treated spots. In this way sets for various concentrations of the compounds were prepared. The slides were left for 24 hours under humid conditions. Finally, one drop of a cotton blue-lactophenol mixture was added to each spot to fix the germinated spores. The number of spores germinated compared to the control was calculated considering an average of 500 spores per treatment. The percentage of inhibition with respect to the control was calculated using the Vincent equation:[11]

$$\text{inhibition} = \frac{C - T}{T} \times 100\%$$

where C is the number of spores germinated in control and T is the total number of spores germinated after treatment. The percentage of spores inhibited from germination were determined at different concentrations. From these, the effective doses for 50% inhibition, ED_{50}, were calculated in units of $\mu g\ l^{-1}$.

Phytotoxicity of the tin compounds were determined on healthy rice seeds of PUSA-2-21 variety, collected from Chinsurah Rice Research Institute, Hooghly, West Bengal.

Rice seeds were dipped in suspensions of the compounds of different concentrations (25, 50 and 100 $\mu g\ ml^{-1}$) for 1, 4 and 8 hours. The treated seeds were allowed to germinate sowed over a mat of moist filter papers arranged in covered petriplates. One hundred seeds were treated for each experiment. After seven days the germinated seeds were counted against the control and those seeds which had produced a coleoptile were considered as germinated. Each experiment was repeated in triplicate. All apparatus and materials were sterilized where necessary using standard procedures.

DISCUSSION

Synthesis and Spectroscopy

The $R_3Sn(O_2CCH_2N(H)C(O)NH_2)$, R = Ph, c-Hex and nBu, compounds have been prepared in moderate yield from the respective reactions of the triorganotin hydroxides (R = Ph, c-Hex) and oxides (R = nBu) with hydantoic acid; physical data are collected in Table 1.

The ^1H NMR chemical shifts of the resonances, and their integration, observed in the spectra (Table 5) confirm the stoichiometry of the compounds. The assignments of the

important absorptions in the infrared spectra of the new compounds are collected in Table 6. The NH_2 and NH stretching frequencies appear between 3480 and 3120 cm^{-1} in a CsI matrix. The spectra are rather complicated in the region 1650 to 1500 cm^{-1} owing to the presence of amide I, amide II and carboxylate streching frequencies. Considering hydantoic acid to be a mono substituted derivative of urea, i.e. $RHNC(=O)NH_2$, following the literature precedent,[12] in each case the NH_2 deformation and C=O stretching vibrations appear together as very strong, but slightly broad bands; in solution these split (Table 6). The amide I (CO) band in $Ph_3(O_2CCH_2N(H)C(O)NH_2)$ occurs at 1555 cm^{-1}, a clear indication that the N-C(=O)-N carbonyl group is involved in coordination in contrast to the other R = c-Hex and R = nBu derivatives for which the equivalent frequencies occur at 1580 and 1585 cm^{-1}, respectively in the solid state. The crystal determination of R = Ph and R = c-Hex compounds have been undertaken to examine in detail the mode of coordination of the hydantoate ligands.

Crystal structures

[$Ph_3Sn(O_2CCH_2N(H)C(O)NH_2)$]

The structure of [$Ph_3Sn(O_2CCH_2N(H)C(O)NH_2)$] is shown in Fig. 1 and selected interatomic parameters are collected in Table 7. The crystallographic asymmetric unit is comprised of two independent [$Ph_3Sn(O_2CCH_2N(H)C(O)NH_2)$] entities, labelled a and b, that do not differ significantly from eachother. The structure is polymeric owing to the presence of bridging hydantoate ligands. The carboxylate end of the hydantoate anion coordinates a tin atom via one oxygen atom only whereas the other end coordinates another tin atom via the carbonyl group. The Sn(1)...O(2a) and Sn(2)...O(2b) separations of 3.544(3) and 3.549(3) Å, respectively are not representative of significant interactions and the same is true for the Sn(1)...N(4b) and Sn(2)...N(4a) separations of 3.861(4) and 3.886(3) Å, respectively. The coordination geometry about each tin atom is completed by the ipso carbon atoms derived from three phenyl groups which define an equatorial plane in

the distorted trigonal bipyramidal environments about the tin atoms. In this description, the Sn(1) [Sn(2)] atom lies 0.1093(3) Å [0.0965(3)Å] out of the trigonal plane in the direction of the carboxylate O(1) atom. The Sn-O separations are non-equivalent with the Sn-O(carboxylate) distances of 2.174(2) and 2.174(2) Å, respectively being significantly shorter than the Sn-O(carbonyl) interactions of 2.319(2) and 2.315(2) Å, respectively; the axial angles are 175.63(8) and 177.4(1)°, respectively. The dihedral angles formed between the three phenyl groups, i.e. C(11-16), C(21-26), and C(31-36), are 93.8, 108.6 and 115.8°, respectively (81.4, 113.6 and 124.6°, respectively for molecule b). In the lattice the polymeric chains are associated via significant hydrogen bonding contacts. Each of the non-coordinating carbonyl groups forms two O...H-N interactions such that O(2a)...H(4b1) is 2.01 Å (the O(2a)...N(4b) separation is 2.901(4) Å and the O(2a)...H-N(4b) angle is 151°) and O(2a)...H(3b) is 2.11 Å (O2(a)...N(3b) 2.977(4) Å and O(2a)...H-N(3b) is 148°) and for molecule b, O(2b)...H(4a1) is 2.11 Å (symmetry operation: 0.5-x, -0.5+y, 0.5-z, O(2b)...N(4a) is 2.920(4) and O(2b)...H-N(4a) is 140°) and O(2b)...H(3a) is 2.19 Å (O(2b)...N(3a) is 3.005(4) Å and O(2b)...H-N(3a) is 141°). The H(4a2) and H(4b2) atoms do not participate in significant hydrogen bonding contacts. The polymeric structure found for [$Ph_3Sn(O_2CCH_2N(H)C(O)NH_2)$] constrasts the monomeric structure found for the R = c-Hex analogue.

[$c\text{-}Hex_3Sn(O_2CCH_2N(H)C(O)NH_2)$]

The molecular structure of [$c\text{-}Hex_3Sn(O_2CCH_2N(H)C(O)NH_2)$] is shown in Fig. 2 and selected interatomic parameters are collected in Table 7. The hydantoate anion coordinates the tin atom via one of the carboxylate oxygen atoms forming a Sn-O(1) interaction of 2.090(4) Å; this separation is shorter than the comparable bonds in the R = Ph derivative. The Sn...O(2) separation of 2.948(5) Å is not indicative of a significant interaction between these atoms. The absence of other significant inter- or intra-molecular interactions involving the tin atom confirms the monodentate mode of coordination of the

hydantoate ligand. The tin atom environment is thus distorted tetrahedral with the maximum distortion from the ideal tetrahedral geometry being manifested in the C(11)-Sn-C(31) angle of 125.6(3) Å which may be traced to the proximity of the non-coordinating O(2) atom. As for the R = Ph derivative there are significant intermolecular hydrogen bonding contacts in the lattice, this time involving both the O(2) and O(4) atoms, the latter owing to the non-coordination of this atom to tin; in this structure all three acidic hydrogen atoms participate in hydrogen bonding. The O(2)...H(4a) separation is 2.06 Å (symmetry operation; 1.5-x, 0.5+y, 0.5-z, the O(2)...N(4) separation is 3.010(7) Å and the O(2)...H-N(4) angle is 168°), O(4)...H(4b) is 2.10 Å (symmetry operation: 1.5-x, -0.5+y, 0.5-z, O(4)...N(4) is 2.993(7) Å and O(4)...H-N(4) is 153°) and O(4)...H(3) is 2.19 Å (symmetry operation: 1.5-x, -0.5+y, 0.5-z, O(4)...N(3) is 3.058(7) Å and O(4)...H-N(3) is 149°).

Hydantoate coordination

The different modes of coordination of the hydantoate ligands in the R = Ph and R = c-Hex structures are reflected in systematic variations of the derived interatomic parameters (Table 7). The ligands in molecule a and b of the R = Ph structure and in the R = c-Hex structure are essentially planar as reflected in the O(1)/C(1)/C(2)/N(3), C(1)/C(2)/N(3)/C(4) and C(2)/N(3)/C(4)/O(4) torsion angles (Table 7). The shorter Sn-O(1) interaction in the R = c-Hex compound leads to a longer C(1)-O(1) bond, i.e. 1.299(6) Å vs 1.277(4) Å (molecule a) and 1.269(4) Å (molecule b), and, concomittantly, shorter C(1)-O(2) interactions, i.e. 1.205(7) Å vs 1.227(4) and 1.222(4) Å, respectively in the R = Ph structure. Other changes in the ligand parameters relate in particular to the C(4)-N(4) and C(4)-O(4) interactions. The carbonyl C(4)-O(4) bond distance of 1.220(7) Å in the R = c-Hex structure is shorter owing to the non participation in coordination to tin of this group compared to the situation observed in the R = Ph structure where elongation of this bond is apparent, i.e. 1.243(4) and 1.252(4) Å. As a consequence of the increased bond order of the C(4)-O(4) bond in the

R = c-Hex structure, the C(4)-N(4) bond distance is increased [1.352(8) Å] compared to that found in the R = Ph structure [i.e. 1.334(4) and 1.326(4) Å].

General Comments

The structure reported here for [$Ph_3Sn(O_2CCH_2N(H)C(O)NH_2)$] is similar to several other triorganotin carboxylates in which the carboxylate residue contains additional potential donor atoms such as oxygen and nitrogen.[13] The closely related structure [$Ph_3Sn(O_2C(CH_2)_2N(H)C(O)NH_2)$] [14] adopts this same motif with important parameters Sn-O(1) 2.143(2), Sn-O(4) 2.352(2) Å and O(1)-Sn-O(4) 171.5(1)°. This motif is similar to that found for many [$R_3Sn(O_2CR')$] structures where the carboxylate is bidentate bridging, i.e. the trans-R_3SnO_2 motif. The other major structural form found for the [$R_3Sn(O_2CR')$] compounds is the isolated, distorted tetrahedral arrangement as seen in the structure of [c-$Hex_3Sn(O_2C(CH_2)_2N(H)C(O)NH_2$].

The observation in the present study of different modes of coordination of the hydantoate ligand leading to disparate structural motifs has many precendents in the structural chemistry of organotin carboxylates. It has been highlighted in recent reviews of the subject that very different structures may be found for closely related chemical formulae.[13] No consistent correlation between steric and/or electronic effects associated with the organotin centre and the nature of the structure adopted ultimely in the solid state has been established thus far, however. The presence of multiple potential hydrogen bonding sites in the hydantoate ligand is another factor that may influence the nature of the structure.[15] It is likely that there is a subtle interplay between all of these factors, as well as the less well defined crystal packing effects, which is responsible for the observed structural variations. It is also noteworthy that the phenomenon of structural diversity found in the organotin carboxylates is indeed found in other main group element system.[16,17]

Biocidal activity

The results of the fungitoxicity and phytotoxicity studies are presented in Tables 8 and 9, respectively. Rice seed germination studies showed that the R = c-Hex and R = Ph derivatives have practically no phytotoxicity but that the R = nBu derivative is comparatively more phytotoxic.

From Table 9 it may be seen that the R = nBu derivative is the most effective against the fungi used in vitro. The fungiotoxicities (ED_{50} values) of the $R_3Sn(O_2CCH_2N(H)C(O)NH_2)$ compounds are in the following order:

$$R = nBu > Ph > c\text{-}Hex$$

Acknowledgements. One of us (Sk. K.) is thankful to the University of North Bengal for the award of a J.R.F. and the Australian Research Council is thanked for support of the crystallographic facility.

References.

1. Crowe, A J Appl. Organomet. Chem., 1987, 1: 143
2. Crowe, A J Appl. Organomet. Chem., 1987, 1: 331
3. Bergon, M and Colmo, J P J. Chem. Soc., Perkin Trans II, 1978, 193
4. Chakrabarti, A, Kamruddin, Sk, Chattopadhyaya, T K, Roy, A, Chakraborty, B N, Molloy, K C and Tiekink, E R T Appl. Organomet. Chem., 1995, 9: 357
5. Ingham, R K, Rosenberg, S D and Gilman, H Chem. Rev., 1960, 60: 490
6. teXsan, Single Crystal Structure Analysis Package, Molecular Structure Corporation, The Woodlands, Texas, 1992
7. Walker, N and Stuart, D Acta Crystallogr., 1983, A39: 158
8. Sheldrick, G M SHELXS86, Program for the Automatic Solution of Crystal Structure, Göttingen, Germany, 1986
9. Johnson, C K ORTEPII, Report 5136, Oak Ridge National Laboratory, TN, 1976
10. Rouxel, T, Sarniget, A, Kollmann, A and Bousquet, J F Physio. Mol. Plant Pathol., 1989, 34: 507
11. Vincent, J K Nature, 1947, 159: 850
12. Bellamy, L J The Infrared Spectra of Complex Molecules, Vol. 1 (3rd Edn), 1975 Chapman and Hall (London).
13. Tiekink, E R T Appl. Organomet. Chem., 1991, 5: 1; Research Trends in Organometallic Chemistry, 1995, in press
14. Lo, K-M, Kumar Das, V G, Yip, W-H and Mak, T C W J. Organomet. Chem., 1991, 412: 21.
15. Ng, S W, Kuthubutheen, A J, Kumar Das, V G, Linden, A and Tiekink, E R T Appl. Organomet. Chem., 1994, 8: 37
16. Tiekink, E R T Main Group Metal Chem., 1992, 15: 161
17. Tiekink, E R T and Winter, G Rev. Inorg. Chem., 1992, 12: 183.

Table 1 Physical data for $R_3Sn(O_2CCH_2N(H)C(O)NH_2)$

Compound	Yield (%)	M. pt (°C)	λ_{max} (nm) [a]	Elemental analysis (%)[b] C	H	N	Sn
R = Ph [c]	40	203	208	53.8 (54.0)	3.9 (4.3)	5.9 (6.0)	25.3 (25.4)
R = c-Hex [d]	50	194	210	53.7 (52.0)	7.5 (7.8)	6.4 (5.8)	23.9 (24.5)
R = nBu [d]	65	112	204	44.4 (44.3)	7.7 (7.9)	7.0 (6.9)	29.1 (29.2)

[a] Spectra recorded in methanol solution. [b] Calculated values in parentheses. [c] recrystallized from methanol solution. [d] recrystallized from $CHCl_3$-petroleum ether (60-80 °C) solution.

Table 2 Crystallographic data for [$Ph_3Sn(O_2CCH_2N(H)C(O)NH_2)$] (**1**) and [c-$Hex_3Sn(O_2CCH_2N(H)C(O)NH_2)$] (**2**)

	1	**2**
Formula	$C_{21}H_{20}N_2O_3Sn$	$C_{21}H_{38}N_2O_3Sn$
Formula weight	467.1	485.2
Crystal system	monoclinic	monoclinic
Space group	$P2_1/n$	$P2_1/n$
a, Å	16.955(6)	10.718(4)
b, Å	14.954(3)	9.088(3)
c, Å	17.865(2)	22.549(6)
β, deg.	115.08(1)	98.49(2)
V, $Å^3$	4102(1)	2268(1)
Z	8	4
D_{calcd}, g cm^{-3}	1.512	1.421
F(000)	1872	1008
μ, cm^{-1}	12.67	11.48
Crystal size, mm	0.23 x 0.48 x 0.48	0.08 x 0.13 x 0.32
Transmission coefficients	0.939 - 1.029	0.870 - 1.056
No. data measured	10199	5803
No. unique data	9879	5517
No. observed data	6839	3188
R	0.033	0.049
R_w	0.035	0.057
ρ_{max}, e $Å^{-3}$	0.48	0.88

Table 3 Fractional atomic coordinates for [$Ph_3Sn(O_2CCH_2N(H)C(O)NH_2)$]

Atom	x	y	z
Sn(1)	0.24925(2)	0.12325(2)	0.17665(1)
Sn(2)	0.28465(2)	0.19923(2)	-0.31119(1)
O(1a)	0.2692(2)	0.1617(2)	0.0686(1)
O(1b)	0.2963(2)	0.1506(2)	0.5793(1)
O(2a)	0.2768(2)	0.3111(2)	0.0691(1)
O(2b)	0.2469(2)	0.0101(2)	0.5581(1)
O(4a)	0.2686(2)	0.2565(2)	-0.1981(2)
O(4b)	0.2275(2)	0.0711(2)	0.2887(1)
N(3a)	0.2839(2)	0.3154(2)	-0.0780(2)
N(3b)	0.2453(2)	0.0050(2)	0.4072(2)
N(4a)	0.2924(3)	0.4058(2)	-0.1763(2)
N(4b)	0.2181(3)	-0.0801(2)	0.2945(2)
C(1a)	0.2751(2)	0.2374(2)	0.0382(2)
C(1b)	0.2688(3)	0.0799(2)	0.5368(2)
C(2a)	0.2794(3)	0.2294(2)	-0.0440(2)
C(2b)	0.2649(4)	0.0884(3)	0.4508(2)
C(4a)	0.2808(2)	0.3237(2)	-0.1535(2)
C(4b)	0.2298(3)	0.0009(2)	0.3277(2)
C(11a)	0.1526(2)	0.2204(2)	0.1634(2)
C(11b)	0.3874(3)	0.1216(3)	-0.2230(2)
C(12a)	0.1422(3)	0.2520(3)	0.2319(2)
C(12b)	0.4397(3)	0.1553(3)	-0.1454(3)
C(13a)	0.0788(3)	0.3142(3)	0.2238(3)
C(13b)	0.5035(4)	0.1031(5)	-0.0868(3)
C(14a)	0.0247(3)	0.3452(3)	0.1468(4)
C(14b)	0.5165(4)	0.0178(5)	-0.1049(3)
C(15a)	0.0346(3)	0.3155(3)	0.0789(3)
C(15b)	0.4667(4)	-0.0166(3)	-0.1808(3)
C(16a)	0.0981(3)	0.2538(3)	0.0867(2)
C(16b)	0.4022(3)	0.0351(3)	-0.2402(3)
C(21a)	0.3818(3)	0.1409(2)	0.2602(2)

C(21b)	0.1534(3)	0.1576(3)	-0.3559(2)
C(22a)	0.4232(3)	0.0799(3)	0.3226(3)
C(22b)	0.1215(3)	0.1164(3)	-0.3055(3)
C(23a)	0.5096(3)	0.0899(4)	0.3776(3)
C(23b)	0.0357(4)	0.0839(4)	-0.3374(4)
C(24a)	0.5560(4)	0.1622(4)	0.3706(3)
C(24b)	-0.0171(4)	0.0922(5)	-0.4188(4)
C(25a)	0.5170(4)	0.2228(4)	0.3093(4)
C(25b)	0.0131(4)	0.1320(5)	-0.4701(4)
C(26a)	0.4303(3)	0.2120(3)	0.2535(3)
C(26b)	0.0978(3)	0.1643(4)	-0.4396(3)
C(31a)	0.2050(3)	-0.0019(2)	0.1183(2)
C(31b)	0.3106(3)	0.3296(2)	-0.3423(2)
C(32a)	0.1193(3)	-0.0274(3)	0.0917(3)
C(32b)	0.3921(4)	0.3548(3)	-0.3300(3)
C(33a)	0.0917(4)	-0.1104(4)	0.0563(3)
C(33b)	0.4089(5)	0.4395(4)	-0.3526(4)
C(34a)	0.1485(5)	-0.1674(3)	0.0450(3)
C(34b)	0.3416(7)	0.4980(4)	-0.3883(4)
C(35a)	0.2329(4)	-0.1435(3)	0.0697(3)
C(35b)	0.2607(6)	0.4751(4)	-0.4003(3)
C(36a)	0.2614(3)	-0.0608(3)	0.1064(2)
C(36b)	0.2437(4)	0.3916(3)	-0.3782(3)

Table 4 Fractional atomic coordinates for [c-$Hex_3Sn(O_2CCH_2N(H)C(O)NH_2)$]

Atom	x	y	z
Sn	0.23034(4)	0.28672(5)	0.11052(2)
O(1)	0.3303(3)	0.1051(5)	0.1479(2)
O(2)	0.4916(4)	0.2549(5)	0.1691(2)
O(4)	0.6864(5)	-0.1946(5)	0.2505(2)
N(3)	0.6393(4)	0.0397(5)	0.2243(2)
N(4)	0.8226(5)	-0.0133(6)	0.2819(3)
C(1)	0.4474(5)	0.1329(7)	0.1679(3)
C(2)	0.5223(5)	-0.0007(7)	0.1897(3)
C(4)	0.7140(6)	-0.0643(7)	0.2518(3)
C(11)	0.3267(5)	0.3339(7)	0.0386(3)
C(12)	0.2353(6)	0.3945(8)	-0.0129(3)
C(13)	0.3039(7)	0.4294(8)	-0.0637(3)
C(14)	0.3718(7)	0.2962(8)	-0.0816(3)
C(15)	0.4613(7)	0.2344(9)	-0.0321(3)
C(16)	0.3968(7)	0.1998(8)	0.0196(3)
C(21)	0.0556(5)	0.1678(7)	0.0874(3)
C(22)	-0.0485(6)	0.2578(9)	0.0517(3)
C(23)	-0.1706(6)	0.1689(9)	0.0372(4)
C(24)	-0.2157(6)	0.1121(10)	0.0899(4)
C(25)	-0.1148(7)	0.0190(9)	0.1252(4)
C(26)	0.0064(6)	0.1082(8)	0.1405(3)
C(31)	0.2111(10)	0.4376(12)	0.1809(4)
C(32)	0.0922(9)	0.5282(12)	0.1740(5)
C(33)	0.0787(12)	0.6250(16)	0.1279(6)
C(34)	0.1717(13)	0.7407(15)	0.1342(6)
C(35)	0.2867(14)	0.6914(16)	0.1308(6)
C(36a)[a]	0.3474(10)	0.5969(13)	0.1723(5)
C(36b)[a]	0.3058(16)	0.5072(21)	0.2051(7)

[a] site occupancy factor = 0.5.

Table 5 ^{1}H NMR data (ppm) for $R_3Sn(O_2CCH_2N(H)C(O)NH_2)$

Compound	δ Sn-aromatic/ ligand ring	δ (NH)	δ (NH_2)	δ (CH_2)	δ (Sn nBu)	δ (Sn c-Hex)
R = Ph [a]	7.96 - 7.06 (m, 15H)	5.96 (b, 1H)	5.48 (s, 2H)	3.62 (d, 2H, J = 5 Hz)		
R = nBu [b]		5.06 (t, 1H, J = 5 Hz)	5.02 (s, 2H)	3.97 (d, 2H, J = 5 Hz)	2.20 - 0.20 (m, 27H)	
R = c-Hex [b]		5.66 (b, 1H)	4.77 (s, 2H)	4.03 (d, 2H, J = 5 Hz)		2.30 - 0.63 (m, 33H)

[a] Spectra recorded in saturated solutions of d_6-DMSO [b] and $CDCl_3$ solution using internal TMS as reference. All shifts are in ppm downfield to TMS. Proton integration are in parentheses. Abbreviations: s = singlet, d = doublet, m = complex multiplet pattern centred at the given δ value, b = broad, t = triplet centred at the given δ value.

Table 6 Selected IR data (cm^{-1}) for $R_3Sn(O_2CCH_2N(H)C(O)NH_2)$

Compound	$\upsilon(NH_2)$	υ(NH)	υ(amide II) $\upsilon(NH_2)$	$\upsilon(NH_2)$	υ(OCO)	υ(amide I) CO	υ(SnC)
R = Ph[a,b]	3415 m 3310 m, b	3260 sh, m 3120 w	1525 s	1555 vs, b	1600 s, b	1555 vs, b	280 w 250w
R = nBu[a]	3480 m 3320 m	3300 sh, m 3180 m	1530 vs, b	1585 vs, b	1620 vs	1585 vs, b	480 w 430 w
R = nBu[c]	3460 s 3340 s	3100 s, b	1525 s, sh	1565 s, b	1620 vs	1650 vs, b	500 w 470 w
R = c-Hex[a]	3430 m 3340 m	3270 m 3150 m	1525 s, b	1580 vs, b	1615 s, b	1580 vs, b	500 w 470 w
R = c-Hex[c]	3440 m, sh 3380 m, b	3280 m 3230 m	1510 m, b	1565 s	1615 s	1630 s, b	500 w, b 425 w

[a] Spectra recorded in CsI optics. [b] The solution spectrum of R = Ph compound was not recorded in solution owing to its poor solubility.

[c] Spectra recorded in $CDCl_3$ solution. Abbreviations: v = very, s = strong, m = medium, w = weak, b = broad, sh = shoulder.

Table 7 Selected bond distances (Å) and angles (°) for $R_3Sn(O_2CCH_2N(H)C(O)NH_2)$

Parameter	R = Ph molecule a	R = Ph molecue b	R = c-Hex
Sn-O(1)	2.174(2)	2.174(2)[a]	2.090(4)
Sn-O(4)	2.319(2)[b]	2.315(2)[c]	
Sn-C(11)	2.127(4)	2.131(4)	2.153(6)
Sn-C(21)	2.122(4)	2.114(5)	2.161(6)
Sn-C(31)	2.118(3)	2.124(4)	2.19(1)
C(1)-O(1)	1.277(4)	1.269(4)	1.299(6)
C(1)-O(2)	1.227(4)	1.222(4)	1.205(7)
C(4)-O(4)	1.243(4)	1.252(4)	1.220(7)
C(2)-N(3)	1.439(4)	1.434(5)	1.438(7)
C(4)-N(3)	1.334(4)	1.331(4)	1.342(7)
C(4)-N(4)	1.334(4)	1.326(4)	1.352(8)
C(1)-C(2)	1.508(5)	1.514(5)	1.503(8)
O(1)-Sn-O(4)	175.63(8)[b]	177.4(1)[a,c]	
O(1)-Sn-C(11)	97.1(1)	97.2(1)[a]	102.3(2)
O(1)-Sn-C(21)	94.3(1)	92.5(1)[a]	94.7(2)
O(1)-Sn-C(31)	87.3(1)	87.9(1)[a]	106.0(3)
O(4)-Sn-C(11)	85.9(1)[b]	85.3(1)[c]	
O(4)-Sn-C(21)	86.7(1)[b]	86.8(1)[c]	
O(4)-Sn-C(31)	88.5(1)[b]	90.1(1)[c]	
C(11)-Sn-C(21)	122.0(1)	121.2(1)	113.6(2)
C(11)-Sn-C(31)	117.0(1)	119.9(2)	125.6(3)

C(21)-Sn-C(31)	120.3(1)	118.2(2)	109.2(3)
Sn-O(1)-C(1)	132.9(2)	131.8(2)	114.0(4)
Sn-O(4)-C(4)	141.7(2)[b,d]	143.9(2)[c,e]	
C(2)-N(3)-C(4)	121.5(3)	121.0(3)	120.2(5)
O(1)-C(1)-O(2)	126.7(3)	127.5(3)	122.9(6)
O(1)-C(1)-C(2)	112.8(3)	112.5(3)	114.0(5)
O(2)-C(1)-C(2)	120.5(3)	120.0(3)	123.1(5)
N(3)-C(2)-C(1)	111.9(3)	112.3(3)	111.4(5)
O(4)-C(4)-N(3)	119.8(3)	120.1(3)	123.1(6)
O(4)-C(4)-N(4)	123.7(3)	123.6(3)	122.2(6)
N(3)-C(4)-N(4)	116.5(3)	116.3(3)	114.7(6)
O(1)/C(1)/C(2)/N(3)	178.7(3)	172.0(4)	-165.1(5)
C(1)/C(2)/N(3)/C(4)	-174.2(3)	172.7(4)	174.0(6)
C(2)/N(3)/C(4)/O(4)	4.3(6)	-3.9(7)	-2(1)

[a] Atom related by the symmetry operation: x, y, -1+z. [b] O(4b). [c] O(4a). [d] C(4b). [e] C(4a).

Table 8 Effect of on the $R_3Sn(O_2CCH_2N(H)C(O)NH_2)$ compounds on spore germination

Spore	R	ED_{50} (mg/ml)
A. alternata	c-Hex	100.00
	Ph	20.00
	nBu	0.50
H. aativum	c-Hex	595.60
	Ph	1.42
	nBu	0.32
H. maydis	c-Hex	22.40
	Ph	3.55
	nBu	0.005
P. oryzae	c-Hex	94.40
	Ph	0.45
	nBu	0.005

Table 9 Effect of on the $R_3Sn(O_2CCH_2N(H)C(O)NH_2)$ compounds on rice seed germination

R	concentration (μg/ml)	% of germinated seeds[a] after treatment for 1 h	4 h	8 h
c-Hex	100	95	93	90
	50	95	93	93
	25	95	95	94
Ph	100	94	92	91
	50	95	94	94
	25	95	95	95
nBu	100	84	81	79
	50	87	83	83
	25	87	85	84
control		95	95	95

[a] with respect to the control.

Captions to Figures

Figure 1 A portion of the polymeric structure and crystallographic numbering scheme for [$Ph_3Sn(O_2CCH_2N(H)C(O)NH_2)$].

Figure 2 The molecular structure and crystallographic numbering scheme for [$c\text{-}Hex_3Sn(O_2CCH_2N(H)C(O)NH_2)$].

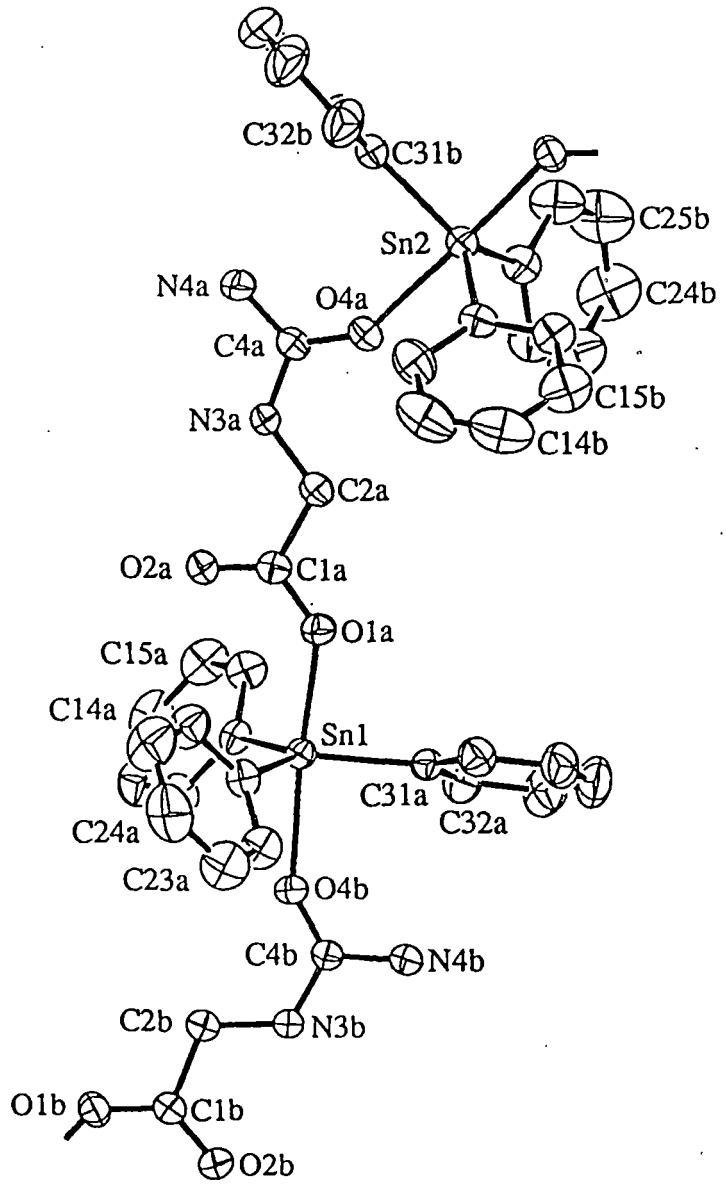

Figure 1 A portion of the polymeric structure and crystallographic numbering scheme for $[Ph_3Sn(O_2CCH_2N(H)C(O)NH_2)]$.

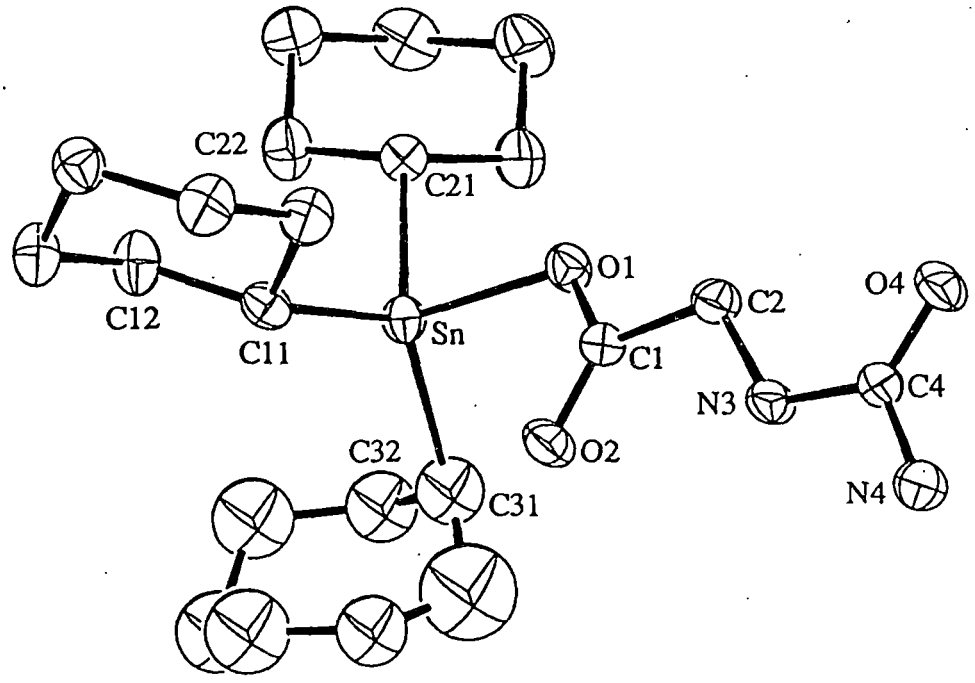

Figure 2 The molecular structure and crystallographic numbering scheme for [c-$Hex_3Sn(O_2CCH_2N(H)C(O)NH_2)$].

APPLIED ORGANOMETALLIC CHEMISTRY, VOL. 9, 357–364 (1995)

Biocidal Organotin Compounds: Part 1. Preparation and Characterization of Triorganotin(IV) 4-Pyridyl- and 2-Pyrimidyl- thioacetates and the Crystal Structure of Triphenyltin(2-pyrimidylthioacetate)

A. Chakrabarti,* Sk. Kamruddin,* T. K. Chattopadhyaya,* A. Roy,* B. N. Chakraborty,† K. C. Molloy‡ and E. R. T. Tiekink§

* Department of Chemistry and † Plant Pathology Laboratory, Department of Botany, University of North Bengal, Darjeeling-734430, India, ‡ School of Chemistry, University of Bath, Claverton Down, Bath, Avon BA2 7AY, UK, and § Department of Chemistry, The University of Adelaide, Adelaide, South Australia 5005, Australia

The preparation and spectroscopic characterization of $[R_3Sn(O_2CCH_2SC_5H_4N\text{-}4)]$, R = Ph, benzyl (Bz), cyclohexyl (c-Hex) and n-Bu, and of $[R_3Sn(O_2CCH_2SC_4H_3N_2\text{-}2,6)]$, R = Me, Ph and n-Bu, are reported. The 2-pyrimidyl compounds feature trigonal bipyramidal tin centres with *trans*-R_3SnO_2 geometries as was confirmed by X-ray crystallography for $[Ph_3Sn(O_2CCH_2SC_4H_3N_2\text{-}2,6]$.¶ By contrast the 4-pyridyl compounds have trigonal bipyramidal geometries in the solid state (arising from intermolecular Sn···N interaction) and tetrahedral geometries in solution. The biocidal activity of these compounds against the fungi *Helminthosporium maydis* (ITCC 2675) and *H. oryzae* (ITCC 2537), both of which damage crops such as maize and rice, shows promise. Encouraging is the observation that the compounds show no adverse phytotoxicity at concentrations to 10^{-3} M.

Keywords: triorganotin; carboxylate; crystal structure; fungitoxicity; Mössbauer

INTRODUCTION

The biocidal properties of organotin carboxylates are very rich[1–3] and in addition these compounds show an interesting range of structural variations[4] leading to structure–activity relationships.[5] These latter studies have shown that triorganotin carboxylates that have either isolated tetrahedral tin centres or *trans*-R_3SnO_2 tin atom geometries (arising from bridging carboxylate ligands) possess significantly greater biocidal activity than the compounds with the monomeric *cis*-R_3SnO_2 structural type, i.e. compounds with chelating carboxylate ligands spanning both equatorial and axial sites.

The above has led to a study of the biocidal activity of a new series of organotin thiocarboxylates,[6] $R_3Sn(O_2CCH_2SR')$, with varying R groups (R = alkyl or aryl) and containing the biologically important 4-pyridyl and 2-pyrimidyl groups incorporated into the carboxylate ligands. This paper details the preparation, spectroscopic characterization and biocidal activity of these compounds and the single-crystal structure determination of a representative compound. During the preparation of this manuscript the crystal structure of $[Ph_3Sn(O_2CCH_2SC_4H_3N_2\text{-}2,6)]$ was reported by others.[7]

EXPERIMENTAL

General

4-Pyridylthioacetic acid and 2-pyrimidylthioacetic acid were procured from Aldrich. The triorganotin halides Me_3SnCl, n-Bu_3SnCl and Ph_3SnCl

§ Author to whom correspondence should be addressed.

¶ Supplementary material is held at the Crystallographic Data Centre, Cambridge, UK.

CCC 0268–2605/95/040357–08

Received 28 September 1994
Accepted 24 February 1995

Table 1 Analytical and UV data for the triorganotin 4-pyridylthio- (R^1) and 2-pyrimidylthio- (R^2) acetates[a]

Compound	Yield (%)	M. pt (°C)	λ_{max} (nm)[a]	Elemental analysis (%)[b] C	H	N	Sn
$Ph_3Sn(O_2CCH_2R^1)$	90	160	214	57.10 (57.94)	3.59 (4.05)	2.58 (2.70)	23.48 (22.92)
$Bz_3Sn(O_2CCH_2R^1)$	92	154	209	59.22 (60.00)	4.10 (4.82)	2.30 (2.50)	20.65 (21.23)
$(c\text{-Hex})_3Sn(O_2CCH_2R^1)$	88	200	217	55.50 (56.00)	7.12 (7.28)	2.52 (2.61)	20.87 (22.15)
$(n\text{-Bu})_3Sn(O_2CCH_2R^1)$	94	85	264	49.71 (49.81)	7.49 (7.20)	3.06 (3.05)	25.38 (25.93)
$Ph_3Sn(O_2CCH_2R^2)$	60	142	228	55.20 (55.52)	3.74 (3.85)	5.36 (5.39)	22.91 (22.83)
$Me_3Sn(O_2CCH_2R^2)$	90	137	248	31.93 (32.46)	4.15 (4.20)	7.98 (8.41)	35.26 (35.67)
$(n\text{-Bu})_3Sn(O_2CCH_2R^2)$	90	53	247	47.30 (47.08)	6.82 (6.97)	5.98 (6.10)	25.68 (25.87)

Abbreviation: Ph, phenyl; Bz, benzyl; c-Hex, cyclohexyl; n-Bu, n-butyl; Me, methyl.
[a] Spectra recorded in methanol solution: [b] Calculated values in parentheses.

were purchased from Aldrich/Fluka AG and were used after crystallization or distillation where necessary. Tribenzyltin chloride was prepared following the literature method.[8] All solvents were purified and dried before use. The reactions were carried out under an inert atmosphere; however, other manipulations were performed under aerobic conditions.

Instrumentation

The IR spectra were recorded on a Pye–Unicam SP-300S spectrophotometer using CsI optics both for solid and solution spectra. ^1H NMR spectra were recorded on a VA-EM-390 90 MHz spectrometer. The UV spectra were recorded on a Shimadzu-240 spectrophotometer. Microanalyses were performed at the National Chemical Laboratory, Pune, India. Tin was estimated gravimetrically as SnO_2.

Syntheses

The sodium salts of 4-pyridylthioacetic acid and 2-pyrimidylthioacetic acid were prepared by titrating a methanolic solution/suspension of the acid with 0.5 M methanolic sodium hydroxide in the presence of an indicator. The sodium salts were isolated as crystals upon concentration of their respective solutions.

The triorganotin(IV) carboxylates were obtained in good yields by refluxing (4–6 h) the appropriate triorganotin chloride with the sodium salts of the carboxylates in methanol solution. The air-stable products were precipitated along with sodium chloride and were purified by recrystallization from acetonitrile. Tables 1–4 summarize the analytical and spectroscopic data for these compounds. The $[Ph_3Sn(O_2CCH_2SC_4H_3N_2\text{-}2,6)]$ compound was also investigated crystallographically.

Crystallography

Intensity data for a colourless crystal (0.16 mm × 0.19 mm × 0.32 mm) were measured at room temperature on a Rigaku AFC6R diffractometer fitted with graphite monochromatized MoKα radiation, $\lambda = 0.71073$ Å, up to θ_{max} 27.5° employing the $\omega:2\theta$ scan technique. The data were corrected for Lorentz and polarization effects[9] and for absorption employing the DIFABS program[10] which resulted in a range of transmission coefficients of 0.856–1.031. Of the 11 442 data measured, 10 906 were unique and 6823 satisfied the $I \geq 3.0\sigma(I)$ criterion of observability and were used in the subsequent analysis.

Crystal data for $C_{24}H_{23}N_2O_2SSn$: $M = 522.2$, monoclinic, space group $P2_1/c$, $a = 21.341(7)$, $b = 11.688(6)$, $c = 19.004(4)$ Å, $\beta = 110.53(2)°$, $V = 4439(5)$ Å^3, $Z = 8$, $D_{calcd} = 1.563$ g cm^{-3}, $F(000) = 2104$, $\mu = 12.68$ cm^{-1}.

The structure was solved by direct methods[11] and refined by a full-matrix least-squares procedure based on *F*.[9] Non-hydrogen atoms were refined with anisotropic thermal parameters and hydrogen atoms were included in the model at their calculated positions (C–H 0.97 Å). At convergence $R = 0.037$ and $R_w = 0.043$ (sigma weights[9]). The analysis of variance showed no special features and the maximum residual in the final difference map was 0.52 e Å^{-3}. The crystallographic numbering scheme used is shown in Fig. 1 (drawn with ORTEP[12]) and selected interatomic parameters are listed in Table 5. Other crystallographic details comprising fractional atomic coordinates, thermal parameters, H-atom parameters, all bond distances and angles, and tables of observed and calculated structure factors are available on request from ERTT.

Biological studies

Virulent cultures of *Helminthosporium maydis* (ITCC 2675) and *H. oryzae* (ITCC 2537), causal agents of brown spot of maize (*Zea mays*) and rice (*Oryzae sativa*), respectively, and *Bacillus cereus* (IMI no. 359387) were obtained from the Plant Pathology Laboratory, Department of Botany, University of North Bengal. Fungi were grown on potato–dextrose–agar (PDA) medium at 28 ± 1 °C, whereas *B. cereus*, isolated from tea leaves (CP-1), were grown on nutrient agar (NA) supplemented with 2 μg ml^{-1} nystatin.

In vitro fungitoxicity was ascertained following spore germination assay as described by Rouxel *et al.*[13] Purified eluents (10 μl) were placed separately at two points 3 cm apart on a clean, grease-free slide. The solvent was allowed to evaporate. One drop of spore suspension (0.02 ml per drop), prepared from 15-day-old cultures of either *H. maydis* or *H. oryzae*, were mounted separately on the glass slide. The slides were incubated on moist Petri plates for 24 h at 25 ± 1 °C. Finally, one drop of a lactophenol–Cotton Blue mixture was added to each spot to fix the germinated spores. The number of spores germinated compared with the control was calculated considering an average of 500 spores per treatment. The percentage of inhibition over the control was calculated using the Vincent equation:[14]

$$\text{Inhibition} = \frac{C - T}{T} \times 100\%$$

where C is the number of spores germinated in control and T is the total number of spores germinated after treatment. From these, the effective

Table 2 Selected IR data (cm^{-1}) for the triorganotin 4-pyridylthio- (R^1) and 2-pyrimidylthio- (R^2) acetates[a]

	Solid				Solution				
Compound	ν_{as}(OCO)	ν_s(OCO)	$\Delta\nu^b$	ν_{as}(SnC)	ν_{as}(OCO)	ν_s(OCO)	$\Delta\nu^b$	ν_{as}(SnC)	ν_s(SnC)
$Na(O_2CCH_2R^1)$	1590 (vs)	1420 (s)	170						
$Ph_3Sn(O_2CCH_2R^1)$	1625 (m)	1320 (s)	305	515 (w)	1640 (m)	1320 (m)	320	550 (m)	490 (m)
$Bz_3Sn(O_2CCH_2R^1)$	1628 (s)	1355 (s)	273	520 (m)	1650 (m)	1320 (m)	330	545 (m)	490 (m)
$(c\text{-Hex})_3Sn(O_2CCH_2R^1)$	1615 (s)	1355 (s)	260	515 (m)	1640 (s)	1315 (m)	325	545 (m)	500 (m)
$(n\text{-Bu})_3Sn(O_2CCH_2R^1)$	1615 (s)	1335 (m)	280	515 (m)	1645 (s)	1320 (s)	—325	545 (m)	490 (m)
$Na(O_2CCH_2R^2)$	1570 (s)	1410 (s)	160						
$Ph_3Sn(O_2CCH_2R^2)$	1575 (s)	1380 (s)	195	515 (m)	1635 (m)	1325 (m)	310	542 (m)	485 (s)
$Me_3Sn(O_2CCH_2R^2)$	1570 (s)	1380 (s)	190	515 (m)	1650 (m)	1325 (m)	325	555 (m)	475 (s)
$(n\text{-Bu})_3Sn(O_2CCH_2R^2)$	1590 (vs)	1400 (s)	190	520 (w)	1630 (s)	1315 (s)	325	550 (m)	495 (m)

Abbreviations: vs, very strong; s, strong; m, medium; w, weak. [a] Spectra recorded in CsI optics, solids in a Nujol mul and solutions in CCl_4. [b] $\Delta\nu = [\nu_{as}(OCO) - \nu_s(OCO)]$ cm^{-1}.

Table 3 ^{1}H NMR data (ppm) for the triorganotin 4-pyridylthio- (R^1) and 2-pyrimidylthio- (R^2) acetates[a,b]

Compound	δ(Sn–aromatic/ligand ring)	δ-(CH_2—)[c]	δ-(CH_2—)[d]	δ-(Sn–alkyl)
$Ph_3Sn(O_2CCH_2R^1)$	8.01 (d)[e] (2H) J = 5 Hz 7.52 (m) (17H)	3.62 (s) (2H)		
$Bz_3Sn(O_2CCH_2R^1)$	8.43 (d)[e] (2H) J = 5 Hz 7.33 (m) (17H)	3.62 (m) (2H)	2.61 (s) (6H) $^2J(^{119}Sn—CH)$ = 63 Hz $^2J(^{117}Sn—CH)$ = 57 Hz	
$(c\text{-}Hex)_3Sn(O_2CCH_2R^1)$	8.55 (d) (2H) J = 5 Hz 7.44 (d) (2H) J = 5 Hz	3.55 (s) (2H)		1.53 (m, b) (33H)
$(n\text{-}Bu)_3Sn(O_2CCH_2R^1)$	8.52 (d) (2H) J = 5 Hz 7.56 (d) (2H) J = 5 Hz	3.54 (s) (2H)		1.31 (m, b) (27H)
$Ph_3Sn(O_2CCH_2R^2)$	8.62 (d) (2H) J = 4 Hz 7.37 (m) (16H)	2.72 (s) (2H)		
$Me_3Sn(O_2CCH_2R^2)$	8.65 (d) (2H) J = 4 Hz 7.51 (t) (1H) J = 4 Hz	2.63 (s) (2H)		0.55 (s) (9H) $^2J(^{119}Sn—CH)$ = 64 Hz $^2J(^{117}Sn—CH)$ = 61 Hz
$(n\text{-}Bu)_3Sn(O_2CCH_2R^2)$	8.34 (d) (2H) J = 4 Hz 7.65 (t) (1H) J = 4 Hz	2.62 (s) (2H)		1.34 (m, b) (27H)

[a] Spectra recorded in saturated solutions of $CDCl_3$ using internal TMS as reference. All shifts are in ppm downfield to TMS. Proton integration in parentheses. [b] Abbreviations: s, singlet; d, doublet; m, complex multiplet pattern centred at the given δ value; b, broad; t, triplet centred at the given δ value. [c] Ligand. [d] Benzyl. [e] The expected second doublet due to ligand protons is masked by the complex multiplet signal patterns of tin–aromatic protons.

doses for 50% inhibition, ED_{50}, were calculated in units of $\mu g\ l^{-1}$.

The fungicidal activity of the compounds was compared with that of triphenyltin acetate[15] (commercially marketed as Fentin acetate).

The bactericidal activity of these compounds was tested following the agar cup bioassay method. Bacterial suspension (1 ml) was mixed with sterilized NA (2 ml per Petri plate) at 45 °C and plated. The plates were chilled for 30 min and then, with the aid of a sterile cork borer, an 8 mm diameter cup was made. The same volume of the solution of the compound was added to each cup and incubated at 37 °C for 24 h. The diameters of the inhibition zones were recorded.

Table 4 ^{119}Sn Mössbauer ($mm\ s^{-1}$) data for selected compounds[a]

Compound	IS	QS	Γ
$Ph_3Sn(O_2CCH_2SC_5H_4N\text{-}4)$	1.20	2.91	0.91, 0.91
$Bz_3Sn(O_2CCH_2SC_5H_4N\text{-}4)$	1.37	2.76	0.92, 0.93
$Ph_3Sn(O_2CCH_2SC_4H_3N_2\text{-}2,6)$	1.26	3.43	0.93, 0.93

[a] Data recorded at 78 K; relative to $CaSnO_3$.

For the study of the phytotoxicity of these compounds, healthy rice seeds of the PUSA-2-21 variety were collected from Chinsurah Rice Research Institute, Hooghly, West Bengal, and were used in the present investigation.

Initially the compounds were dissolved in acetone (2–3 drops), then water suspensions of these compounds were prepared at concentrations of 200, 100, 50 and 25 $\mu g\ ml^{-1}$. Acetone controls for each treatment and one set of water controls were arranged.

Healthy seeds were dipped in the range of water suspensions for each of the compounds tested for 1, 4 and 8 h. The treated seeds were then allowed to germinate, sown over a mat of moist filter papers arranged in covered Petri plates. One hundred seeds were treated for each experiment. After seven days, the germinated seeds were counted; seeds producing a root or

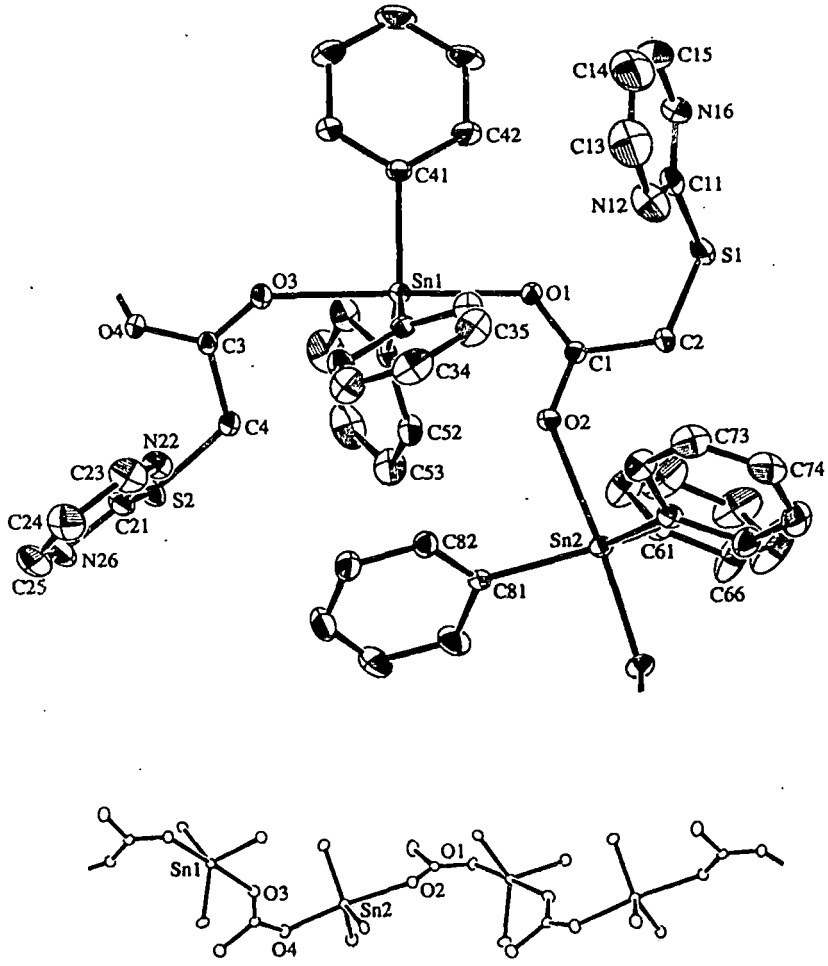

Figure 1 Molecular structure and crystallographic numbering scheme for the two molecules comprising the asymmetric unit in $[Ph_3Sn(O_2CCH_2SC_4H_3N_2\text{-}2,6)]$. The lower view shows the polymeric structure; the R' and all but the *ipso* carbon atoms of the phenyl rings have been omitted for clarity.

coleoptile were considered as germinated. Each experiment (i.e. four concentrations, three time regimes per compound) was repeated in triplicate. All apparatus and materials were sterilized where necessary using standard procedures.

DISCUSSION

Synthesis and spectroscopy

The triorganotin(IV) carboxylates (Table 1) were obtained in good yield via the metathetical reaction between the triorganotin halide and the sodium salts of 4-pyridylthioacetic acid and 2-pyrimidylthioacetic acid.

Infrared data for the compounds are presented in Table 2. The difference in ν_{as}(OCO) and ν_s(OCO) (i.e. $\Delta\nu$) in the solid state for the 4-pyridylthioacetates is quite large, i.e. 260–305 cm^{-1}, whereas $\Delta\nu$ is quite low for the 2-pyrimidylthioacetates, i.e. 190–195 cm^{-1}. These results indicate that the 4-pyridylthioacetate ligands coordinate via one oxygen atom only, as confirmed by an independent crystal structure analysis of $[Ph_3Sn(O_2CCH_2SC_5H_4N\text{-}4)]$.[16] In this structure, a trigonal bipyramidal tin centre was observed owing to the presence of weak intermolecular Sn···N interactions. By contrast, a

bidentate bridging mode is indicated for the 2-pyrimidylthioacetates, as revealed by the X-ray analysis of a representative compound, $[Ph_3Sn(O_2CCH_2SC_4H_3N_2\text{-}2,6)]$ (see below). In solution, the $\Delta\nu$ values for the triorganotin 4-pyridylthioacetate complexes are comparable with those observed in the solid state, suggesting a similar coordination mode. In the case of the 2-pyrimidylthioacetates, the rise in the $\Delta\nu$ values suggests a change in coordination about the tin atom, i.e. from a trigonal bipyramid (solid state) to a tetrahedral geometry (solution). In the solid-state spectra the planarity of the C_3Sn moiety is also indicated by the appearance of only one ν(Sn—C) whereas in solution both ν_{as}(Sn—C) and ν_s(Sn—C) are observed.

The ^1H NMR data are summarized in Table 3. The observed shifts and splittings confirm the stoichiometries of the compounds. For all the compounds studied, the PhSn and the signal due to the protons of the heterocyclic rings appear as complex patterns in the region 8.01 to 7.33 ppm. In the 4-pyridyl series, the δ(Sn—CH_2) for the Bz_3Sn derivative appeared as a singlet at 2.61 ppm [$^2J(^{119}Sn—CH_2) = 63$ Hz and $^2J(^{117}Sn—CH_2) = 57$ Hz], whereas the δ(Sn–cyclohexyl) and δ(Sn–butyl) protons appeared as complex patterns centred about 1.53 and 1.31 ppm, respectively. For the 2-pyrimidyl compounds, Sn—CH_3 resonance appeared as a singlet at δ0.55 ppm with $^2J(^{119}Sn—CH_3) = 64$ Hz and $^2J(^{117}Sn—CH_3) = 61$ Hz.

The $\delta(CH_2)$ of the carboxylate ligands merit special comment. The signals for the CH_2 protons of the 4-pyridylthioacetates appeared at approximately δ3.4–3.6 ppm whereas the corresponding

Table 5 Selected bond distances (Å) and angles (°) for $[Ph_3Sn(O_2CCH_2SC_4H_3N_2\text{-}2,6)]$

Atoms	Distance	Atoms	Distance
Sn(1)—O(1)	2.196 (4)	Sn(2)—O(4)'[a]	2.143 (4)
Sn(1)—O(3)	2.326 (4)	Sn(2)—O(2)	2.323 (4)
Sn(1)—C(31)	2.116 (5)	Sn(2)—C(61)	2.109 (5)
Sn(1)—C(41)	2.114 (5)	Sn(2)—C(71)	2.099 (5)
Sn(1)—C(51)	2.098 (5)	Sn(2)—C(81)	2.098 (6)
S(1)—C(2)	1.772 (6)	S(2)—C(4)	1.768 (6)
S(1)—C(11)	1.726 (7)	S(2)—C(21)	1.730 (6)
O(1)—C(1)	1.254 (6)	O(3)—C(3)	1.237 (6)
O(2)—C(1)	1.235 (6)	O(4)—C(3)	1.240 (6)
N(12)—C(11)	1.286 (9)	N(22)—C(21)	1.298 (7)
N(12)—C(13)	1.35 (1)	N(22)—C(23)	1.321 (8)
N(16)—C(11)	1.324 (9)	N(26)—C(21)	1.321 (8)
N(16)—C(15)	1.34 (1)	N(26)—C(25)	1.35 (1)
C(1)—C(2)	1.504 (7)	C(3)—C(4)	1.506 (7)
C(13)—C(14)	1.32 (2)	C(23)—C(24)	1.34 (1)
C(14)—C(15)	1.31 (2)	C(24)—C(25)	1.35 (1)
O(1)–Sn(1)–O(3)	178.7 (1)	O(2)–Sn–O(4)'	174.0 (1)
O(1)–Sn(1)–C(31)	90.7 (2)	O(2)–Sn(2)–C(61)	90.0 (2)
O(1)–Sn(1)–C(41)	89.8 (2)	O(2)–Sn(2)–C(71)	89.4 (2)
O(1)–Sn(1)–C(51)	94.1 (2)	O(2)–Sn(2)–C(81)	84.8 (2)
O(3)–Sn(1)–C(31)	88.9 (2)	O(4)'–Sn(2)–C(61)	88.1 (2)
O(3)–Sn(1)–C(41)	91.5 (2)	O(4)'–Sn(2)–C(71)	96.6 (2)
O(3)–Sn(1)–C(51)	85.3 (2)	O(4)'–Sn(2)–C(81)	91.3 (2)
C(31)–Sn(1)–C(41)	116.5 (2)	C(61)–Sn(2)–C(71)	114.4 (2)
C(31)–Sn(1)–C(51)	134.7 (2)	C(61)–Sn(2)–C(81)	120.7 (2)
C(41)–Sn(1)–C(51)	108.6 (2)	C(71)–Sn(2)–C(81)	124.5 (2)
C(2)–S(1)–C(11)	103.3 (3)	C(4)–S(2)–C(21)	102.1 (3)
Sn(1)–O(1)–C(1)	124.7 (3)	Sn(2)–O(4)'–C(3)'	131.2 (4)
Sn(1)–O(2)–C(1)	136.7 (3)	Sn(2)–O(3)–C(3)	138.0 (3)
C(11)–N(12)–C(13)	114.6 (9)	C(21)–N(22)–C(23)	115.5 (6)
C(11)–N(16)–C(15)	114.7 (8)	C(21)–N(26)–C(25)	113.8 (6)

[a] Atom related by the symmetry operation: x, 1.5 − y, −0.5 + z.

Table 6 Comparative study of the effect of $R_3Sn(O_2CCH_2SC_5H_4N-4)$ on *Helminthosporium maydis* fungus

Concentration (M)	Germination (%)	
	$(n\text{-}Bu)_3Sn(O_2CCH_2R^1)$[a]	$Ph_3Sn(O_2CCH_2R^1)$[a]
Control	92	92
10^{-3}	0	0
10^{-4}	3	5
10^{-5}	61	40
10^{-6}	84	76
ED_{50}(μg l^{-1})	13	3

[a] R^1 = pyridylthio

signals for the 2-pyrimidylthioacetates appeared at δ2.6–2.7 ppm. The downfield shift for the former complexes is probably due to the fact that the pyridine residue is more electron-withdrawing than the pyrimidine residue, which correlates with the enhanced basicity of the 4-pyridylthioacetates.

A selection of the compounds were also subjected to a tin-119 Mössbauer study. Details of the experimental techniques have been reported previously[17] and data are summarized in Table 4. The slight increase in the isomer shift (IS) value for $[Bz_3Sn(O_2CCH_2SC_5H_4N-4)]$ compared with $[Ph_3Sn(O_2CCH_2SC_5H_4N-4)]$ is due to the reduced electron-withdrawing ability of the benzyl substituents compared with the phenyl groups. The quadrupole splitting (QS) of $[Ph_3Sn(O_2CCH_2SC_4H_3N_2\text{-}2,6)]$ (3.43 mm s^{-1}) is typical of five-coordinate organotin carboxylates incorporating a bridging CO_2 moiety, e.g. $[Me_3Sn(O_2CMe)]$[18,19] has QS = 3.68 mm s^{-1}. The lower QS values for $[Ph_3Sn(O_2CCH_2SC_5H_4N-4)]$ and $[Bz_3Sn(O_2CCH_2SC_5H_4N-4)]$ (2.91 and 2.76 mm s^{-1}, respectively) reflect the asymmetric C_3SnON coordination sphere evident in the structure of $[Ph_3Sn(O_2CCH_2SC_5H_4N-4)]$, for which the Sn···N interaction is weak.[16] The similarity of QS values for each of $[Ph_3Sn(O_2CCH_2SC_5H_4N-4)]$ and $[Bz_3Sn(O_2CCH_2SC_5H_4N-4)]$ suggests similar structures featuring a C_3SnON core in contrast to a C_3SnO_2 core in the structure of $[Ph_3Sn(O_2CCH_2SC_4H_3N_2\text{-}2,6)]$.

Table 7 Comparative study of the effect of $R_3Sn(O_2CCH_2SC_4H_3N_2\text{-}2,6)$ on *Helminthosporium oryzae*

Compound	Concentration (M)	Germination (%)	
$Ph_3Sn(O_2CCH_2R^2)$[a]	10^{-3}	0	
	10^{-4}	32	
	10^{-5}	46	ED_{50} = 60 μg l^{-1}
	10^{-6}	80	
$Ph_3Sn(O_2CCH_2R^2)$[a]	10^{-3}	5	
	10^{-4}	67	
	10^{-5}	86	ED_{50} = 200 μg l^{-1}
	10^{-6}	97	

[a] R^2 = pyrimidinylthio

Crystal structure

The structure of $[Ph_3Sn(O_2CCH_2SC_4H_3N_2\text{-}2,6)]$ is shown in Fig. 1, and selected interatomic parameters are listed in Table 5. The structure reported here for $[Ph_3Sn(O_2CCH_2SC_4H_3N_2\text{-}2,6)]$ is in essential agreement with that reported by others.[7] The crystallographic asymmetric unit comprises two independent $[Ph_3Sn(O_2CCH_2SC_4H_3N_2\text{-}2,6)]$ units which associate as a result of intermolecular Sn→O contacts, afforded by bidentate bridging carboxylate groups, as shown in Fig. 1. The resultant structure is therefore polymeric, as shown in the lower view of Fig. 1. There is no evidence of coordination to tin by either the heterocyclic nitrogen atoms or the thioether atoms. Each of the tin atoms exists in a distorted trigonal bipyramidal geometry with the axial positions occupied by the oxygen atoms and the equatorial plane defined by the three phenyl groups. The Sn(1) atom lies 0.0607(4) Å out of the trigonal plane in the direction of O(1) atom and the corresponding distance for the Sn(2) atom is 0.0751(4) Å, in the direction of the O(4)′ atom (symmetry operation: x, $1.5-y$, $-0.5+z$). The difference in the Sn—O bond distances about each of the tin atoms is relatively small, but experimentally significant, at 0.13 and 0.18 Å for the Sn(1) and Sn(2) atoms, respectively, indicating a relatively symmetrical bridging mode for the carboxylate ligands. The near-equivalence in the Sn—O bond distances is reflected in the narrow range of C—O bond distances of 1.235(6)–1.254(6) Å. There is a notable difference in the C–Sn–C angles about the two tin centres, with the range of angles about the Sn(1) atom being 108.6(2)–134.7(2)° and that about the Sn(2) atom being smaller at 114.4(2)–124.5(2)°. The expansion of the C(31)–Sn(1)–C(51) angle to 134.7(2)° and concomitant contraction of the other two angles from the ideal trigonal values may be traced to the relatively close approach of the O(2) atom, i.e. 3.280(5) Å. The weak

Sn(1)···O(2) contact does not represent a significant bonding interaction, however. Whereas the tin atom geometries are in essential agreement with each other, there are some significant differences in the relative orientations of the tin-bound phenyl substituents and of the pyrimidine residues. The dihedral angles between the C(31)–C(36), C(41)–C(46) and C(51)–C(56) rings of 67.7, 100.6 and 100.4°, respectively, i.e. about the Sn(1) atom, may be compared with the angles of 53.7, 102.7 and 147.8° for the C(61)–C(66), C(71)–C(76) and C(81)–C(86) rings, respectively. For the carboxylate ligands, the C(1)/C(2)/S(1)/C(11) and C(2)/S(1)/C(11)/N(12) torsion angles of 74.5(5) and 17.8(6)°, respectively, are significantly different from the comparable C(3)/C(4)/S(2)/C(21) and C(4)/S(2)/C(21)/N(22) angles of −64.2(5) and −1.1(6)°, respectively.

The structure reported here for $[Ph_3Sn(O_2CCH_2SC_4H_3N_2\text{-}2,6)]$ corresponds to one of the major structural motifs found for compounds with the general formula $[R_3Sn(O_2CR')]$.[4] The other main motif for this formula has a monomeric structure in which the tin atom is four-coordinate (i.e. where the carboxylate ligand is monodentate) or approaching five-coordinate (where the carboxylate ligand is coordinating in an asymmetric mode). There are several other $[R_3Sn(O_2CR')]$ structures available in which an additional atom that is incorporated in the carboxylate residue, e.g. oxygen or nitrogen, is also coordinated to the tin atom giving rise to different motifs;[4] however, as mentioned above, no such intra- or inter-molecular interactions are found in the structure of $[Ph_3Sn(O_2CCH_2SC_4H_3N_2\text{-}2,6)]$.

Fungicidal activity

The results of the fungitoxicity and phytotoxicity tests are summarized in Tables 6 and 7, respectively. No fungitoxicity was found for the 4-pyridylthio- and 2-pyrimidylthio-acetic acids at the 10^{-3} M level, whereas their triorganotin complexes showed increased activity. For the 4-pyridylthioacetates tested against *H. maydis*, the triphenyl derivative was more active than the tributyl species. By contrast, the tributyltin 2-pyrimidylthioacetate compound has greater activity than the triphenyltin derivative at different concentrations against *H. oryzae*. However, the activity of the butyl compound decreases markedly at lower concentrations.

The 100 ppm concentration of Fentin acetate was found to inhibit the growth of the fungi when treated *in vitro* and hence it is encouraging to find that the newly synthesized compounds are potentially more active (see Tables 6 and 7). Further testing, *in vivo*, is required to confirm these results.

The bactericidal activity of all the compounds was such that they killed over 95% of the bacterial *Bacillus cereus* under the conditions of the experiment (results not shown).

Acknowledgement The Austrialian Research Council (ERTT), CSIR and NBU (AC and SK) are thanked for support.

REFERENCES

1. P. Smith and L. Smith, *Chem. Br.* **11**, 209 (1975).
2. G. J. M. van der Kerk, *Chemtech.* 356 (1978).
3. K. C. Molloy, T. G. Purcell, M. F. Mahon and E. Minshall, *Appl. Organomet. Chem.* **1**, 507 (1987).
4. E. R. T. Tiekink, *Appl. Organomet. Chem.* **5**, 1 (1991); *idem, Research Trends in Organometallic Chemistry*, 1994, in press.
5. S. J. Blunden, P. J. Smith and B. Sugavanaman, *Pestic. Sci.* **15**, 253 (1984).
6. J. Holeček, K. Handlíř, A. Lyčka, T. K. Chattopadhyay, B. Majee and A. K. Kumar, *Coll. Czech. Chem. Commun.* **51**, 1100 (1986).
7. S. W. Ng, V. G. Kumar Das, W.-H. Yip and T. C. W. Mak, *J. Cryst. Spectr. Res.* **23**, 441 (1993).
8. K. Sisido, Y. Takeda and Z. Kinugawa, *J. Am. Chem. Soc.* **83**, 538 (1961).
9. *teXsan, Single Crystal Structure Analysis Package*, Molecular Structure Corporation, The Woodlands, Texas, 1992.
10. N. Walker and D. Stuart, *Acta Crystallogr.* Sect. A **39**, 158 (1983).
11. G. M. Sheldrick, *SHELXS86, Program for the Automatic Solution of Crystal Structure*, Göttingen, Germany, 1986.
12. C. K. Johnson, *ORTEPII*, Report 5136, Oak Ridge National Laboratory, TN, 1976.
13. T. Rouxel, A. Sarniget, A. Kollmann and J. F. Bousquet, *Physiol. Mol. Plant Pathol.* **34**, 507 (1989).
14. J. K. Vincent, *Nature (London)* **159**, 850 (1947).
15. B. F. E. Ford, B. V. Liengme and J. R. Sams, *J. Organomet. Chem.* **19**, 53 (1969).
16. S. W. Ng and V. G. Kumar Das, *Acta Crystallogr. Sect. C*, **48**, 2025 (1982).
17. K. C. Molloy, T. G. Purcell, K. Quill and I. W. Nowell, *J. Organomet. Chem.* **267** 237 (1984).
18. H. Chih and B. R. Penfold, *J. Cryst. Mol. Struct.* **3**, 285 (1973).
19. J. N. R. Ruddick and J. R. Sams, *J. Chem. Soc., Dalton Trans.* 470 (1974).